Nuclear Instruments and Methods in Physics Research A 599 (2009) 106–112

Contents lists available at ScienceDirect

Nuclear Instruments and Methods in Physics Research A

journal homepage: www.elsevier.com/locate/nima

# Hadron multiplicity studies on a combined Pb/U-blanket spallation source: Experimental and simulation benchmark analysis

S. Stoulos [a,*], M. Fragopoulou [a], A. Sosnin [b], M. Manolopoulou [a], M. Krivopustov [b], M. Zamani [a]

[a] School of Physics, Aristotle University of Thessaloniki, 541 24 Thessaloniki, Greece
[b] Joint Institute for Nuclear Research, 141980 Dubna, Russia

ARTICLE INFO

*Article history:*
Received 8 July 2008
Received in revised form
29 October 2008
Accepted 31 October 2008
Available online 11 November 2008

*Keywords:*
Spallation sources
Neutron and proton multiplicity
Passive detectors
Transmutation

ABSTRACT

Spallation sources are able to produce intense neutron fluxes using massive targets when irradiated by relativistic proton beams. Such sub-critical Accelerator Driven Systems (ADSystem) can be used for transmutation or incineration of long-lived radioactive waste by neutron captures or neutron induced fission. In the present study a spallation source consisted of a combined Pb/U target was irradiated by relativistic proton beams from 0.7 up to 2 GeV. Neutron fluences were measured using passive detectors. A benchmark analysis was applied on the experimental results taken under consideration Monte Carlo simulation data of neutron multiplicity. In order to evaluate the tolerance of the structural materials in source design, the neutron and proton distributions escaping the source surface were measured. The spallation source performance in terms of neutron and proton production as well as the effectiveness of a polyethylene shielding surrounding the spallation source is also discussed.



## 1. Introduction

Currently there are a growing number of studies trying to address the international concern about safer nuclear energy and management of accumulated nuclear waste by using Accelerator Driven Systems (ADSystem). Such sub-critical assemblies, called spallation sources, are used in order to obtain high-fluxes of neutrons in an extended energy spectrum; from thermal up to particle beam energy. Neutron capture or neutron induced fission reactions are the most efficient way to transmute long-lived isotopes into stable or short-lived elements. Although, both processes occur in a reactor neutron spectrum, the necessity of a hard neutron spectrum combined with controllable criticality leads to the use of ADSystem [1–7]. A detailed engineering design of an ADSystem requires a performance optimization in terms of neutron production as well as an assessment of the radiation field intensity. The neutron spectrum is a decisive factor for source efficiency studies on transmutation or incineration experiments. Due to the high-radiation emitted by a spallation source, an effective shielding against energetic hadrons and photons is required. Particularly, the structural materials have to be carefully chosen so that can tolerate the gas accumulation caused by fast secondary neutrons induced (n,α) reactions and protons, including protons generated by (n,*x*p) or (p,*x*p) reactions [8–11].

Various spallation sources using targets such as Fe, Ni, W, Bi, Pb, Th or U have been constructed and studied worldwide. Several experimental results as well as Monte Carlo simulations in the field of spallation physics and neutron multiplicity have been published during last decades [12–18]. An enhancement of the neutron production from a Pb target can be achieved by the use of additional appropriate materials, such as U. A further neutron multiplication can be obtained because of the high cross-section of fission induced by fast neutrons and spallation reactions in uranium. Additional moderators can be used to further slow down the produced neutrons to the resonance and thermal plus epithermal energy ranges, thus enabling them to transmute long-lived fission products via capture reactions. Based on that frame, a sub-critical electronuclear set-up "Energy plus Transmutation" has been constructed at the Laboratory of High Energies, JINR, Dubna, with the motivation to perform experiments on increasing safety nuclear power engineering and transmutation of radioactive waste [7]. The "E+T" set-up, a Pb target surrounded by a ~8 cm thick U-blanket, was enclosed in a polyethylene shielding. The $^{239}$Pu(n,f), $^{238}$Pu(n,f), $^{237}$Np(n,γ), $^{129}$I(n,γ) transmutation effectiveness has been studied by irradiations with relativistic proton beams [19]. The aim of the current study was to measure the wide energy hadrons' spectrum, emitted by the source. The determination of the neutron and proton fluence was performed by the use of passive methods.

In the present work, the neutron and proton production from the combined Pb/U-blanket spallation source is discussed. Neutron fluences were measured using several types of passive

*Corresponding author. Tel.: +30 231 0998 202; fax: +30 231 0998 205.
*E-mail address:* Stoulos@auth.gr (S. Stoulos).

0168-9002/$ - see front matter © 2008 Elsevier B.V. All rights reserved.
doi:10.1016/j.nima.2008.10.034

detectors i.e. SSNT Detectors (SSNTDs) (as particle and fission detectors) and activation detectors ($^{238}$U, $^{nat}$Au) with complementary detection energy ranges. A benchmark analysis was applied to the experimental and simulation data. The tolerance of the structural materials in source design-construction was assessed by measuring the emitted proton distributions using $^{nat}$Cd activation technique. The spallation source performance in terms of neutron production as well as the effectiveness of a polyethylene shielding is also discussed.

## 2. Experimental

The "Energy plus Transmutation" set-up was a spallation source in which the combined Pb/U-blanket target was consisted of an 8.4 cm in diameter cylindrical Pb core, surrounded by natural U rods of 3.6 cm in diameter and 10.4 cm in length (U-blanket). The U-rods form a hexagon around the target. The set-up is constructed from four identical sections of the combined target with approximately 0.8 cm gap between them and total length 50 cm (Fig. 1a). The "E+T" set-up was surrounded by an external shielding for radiation protection reasons as shown in Fig. 1b. The shielding was consisted of a wood container filled with granulated polyethylene for slowing down high-energy neutrons. The 1 mm thick Cd-neutron absorber located at the inner walls of the container reduced significantly the backscattering thermal plus epithermal neutrons into the target and detectors volume [7]. Proton beams with energies of 0.7, 1.0, 1.5 and 2.0 GeV were delivered from Nuclotron accelerator at Laboratory of High Energies, JINR Dubna. The integrated intensity of the beam was $10^{13}$ protons. Proton beam monitoring was performed using activation foils of aluminium [$^{27}$Al(p,3pn)$^{24}$Na reaction] and copper [Cu(p,$x$) reactions] [20,21].

Hadrons fluence measurements were performed on the surface of U-blanket as well as on top of the polyethylene shielding as indicated in Fig. 1b. On the upper surface of each section of the U-blanket a set of SSNTDs and a set of activation detectors ($^{238}$U, $^{nat}$Au, $^{nat}$Cd) were positioned along the target axis. Sets of SSNTDs were also placed on the upper shielding surface at three different positions perpendicularly to the target axis. These detectors were applied to measure neutrons escaping from the shielding. The advantage of SSNTDs is due to their insensitivity to gamma rays, which are in abundance in the environment of a spallation source. Each set of SSNTDs used for particle detection consisted of a PolyAllylDiglycolCarbonate (PADC) (Pershore Mouldings Standard Grade, PM355) foil on polyethylene plate 0.5 cm in thickness. Half of each foil was covered with $^{6}Li_2B_4O_7$ converter material. That area was partially covered by 1 mm of Cd

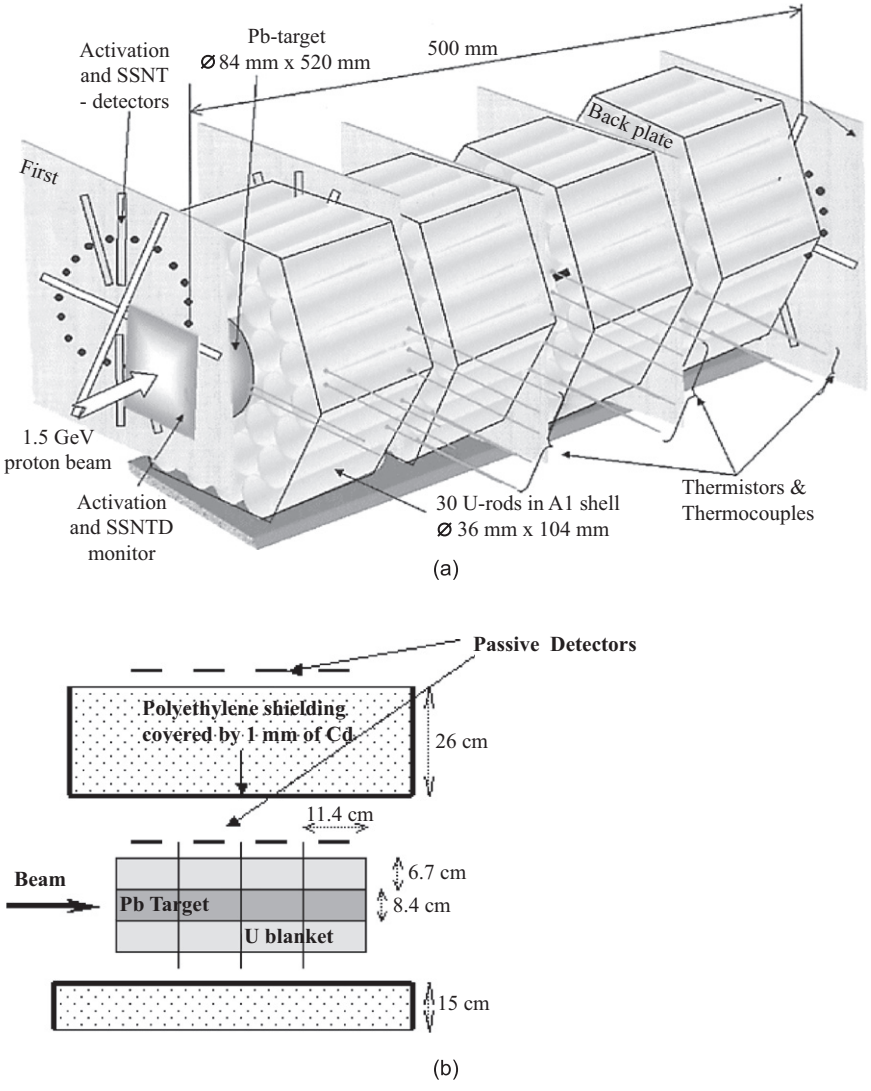


**Fig. 1.** (a) The "Energy plus Transmutation" set-up and (b) longitudinal cross-section of the Pb/U-blanket assembly with passive detector positions.

[22]. The Cd uncovered area responded to the total neutron spectrum while the Cd covered area detected neutrons with energies higher than 1 eV. The track density difference between the Cd-covered and uncovered PADC foil plus $^{6}Li_2B_4O_7$ converter represents the neutron fluence up to 1 eV due to (n,α)-processes induced by thermal plus epithermal neutrons in $^{10}B(n,\alpha)^{7}Li$ and $^{6}Li(n,\alpha)^{3}H$ reactions. The track density on the bare PADC foil originated by proton recoil provided information for intermediate-fast neutrons with about constant response, in the energy range of $0.3 < E_n < 3$ MeV, for the applied etching conditions [23]. A different SSNTD set up was applied to detect fission reactions induced by neutrons using Lexan foils. Fissionable target with a mass of ~300 μg (such as $^{232}Th$) was used for fast neutron (>2 MeV) detection [24]. The applied SSNTDs as particle detectors were irradiated with $10^{11}$ protons while the fission detectors with $10^{13}$ protons in order to achieve a well-measured track density.

The neutron distribution along the target was also determined using activation detectors. Depleted U ($^{235}U/^{238}U$=0.18±0.01%) and natural Au samples (mass ~3 up to 6 mg) were irradiated over the U-blanket measuring the slow neutron fluencies (up to 10 keV) [25]. Natural Cd foils of 1 mm thickness (mass ~2 g, purity 99.9%) were also used as activation detector [26]. The natural Cd foil effectively captures neutrons below 1 eV because of the high cross-section of $^{113}Cd$ capture to thermal plus epithermal neutrons. Cd foil can also be used for neutron detection via the $^{114}Cd(n,\gamma)^{115}Cd$ reaction. Moreover, natural Cd has a significant cross-section to $^{nat}Cd(p,x)^{111}In$ reaction in the energy range of $1\,\text{MeV} \leqslant E_p \leqslant 400$ MeV, responded well to the emitted proton spectrum [16,27]. The activation detectors were irradiated with $10^{13}$ protons in order to obtain a measurement uncertainty lower than 8%.

## 3. Results and discussion

The experimental data were the counted track density from the SSNTDs and radioisotope's concentration from the activation detectors coming from a wide neutron spectrum. In order to convert raw data to neutron fluence, an effective cross-section of the reaction was calculated. For these calculations the neutron and proton energy spectrum was estimated theoretically by using the high-energy transport code DCM–DEM. The DCM–DEM code is a Dubna version of cascade-evaporation approach, similar to Bertini model, taking under consideration high-energy fission and pre-equilibrium emission [28]. The simulation applied at the middle of each section of the U-blanket where the detectors were located. Typical calculated hadrons spectra over each section of the U-blanket are provided in Fig. 2. The ascendancy of neutrons in the energy range from 10 keV up to 20 MeV, peaking at about 0.7 MeV, can be observed. Slow neutron fluence ($E_n < 10$ keV) was found to be less than 12% of the total neutron fluence while only a negligible amount, less than 1% of the total neutron spectrum, corresponded to thermal plus epithermal neutrons ($E_n < 1$ eV). The contribution of neutrons with $E_n > 20$ MeV was found to be less than 2% of the total neutron spectrum. Cross-section data of ENDF/B-*x* [29] were taken into account in order to determine the effective cross-section for each radiator (Table 1). Considering the simulated fluence data, the fraction (%) on the radiator reaction rate was estimated in specific neutron energy ranges as shown in Table 1. The total neutron production was determined using the (n,γ) and (n,α) reactions for slow neutrons, and (n,n′) and (n,f) reactions for intermediate-fast and fast neutron respectively, with an overlap in the region of 2–3 MeV.

The simulated proton fluence was spread in the energy interval of 10 MeV up to 400 MeV (peaking around 60 MeV). This proton fluence, caused by fast neutrons induced proton reactions near the surface of U-blanket, was found to be three orders of magnitude less than the total neutron fluence. According to cross-section data for $^{nat}Cd(p,x)$ reactions [30–32], natural Cd responds to protons with an effective cross-section of 62±11 mb. Corrections due to Cd sample thickness were applied using the Continuous Slow Down Approximation method (ICRU report 49).

### 3.1. Experimental and simulation benchmark analysis

The experimental data show that the neutron fluence at the intermediate-fast region (0.3–3 MeV) spread in the range of $10^{-2}\,\text{cm}^{-2}$ per incoming proton. That fluence was about five times higher than the slow neutron fluence (<10 keV) and almost two times higher compared to fast neutron fluence above 2 MeV. Concerning thermal plus epithermal neutrons, no significant difference in track densities between the Cd-covered and uncovered PADC foil with $^{6}Li_2B_4O_7$ converter was detected.

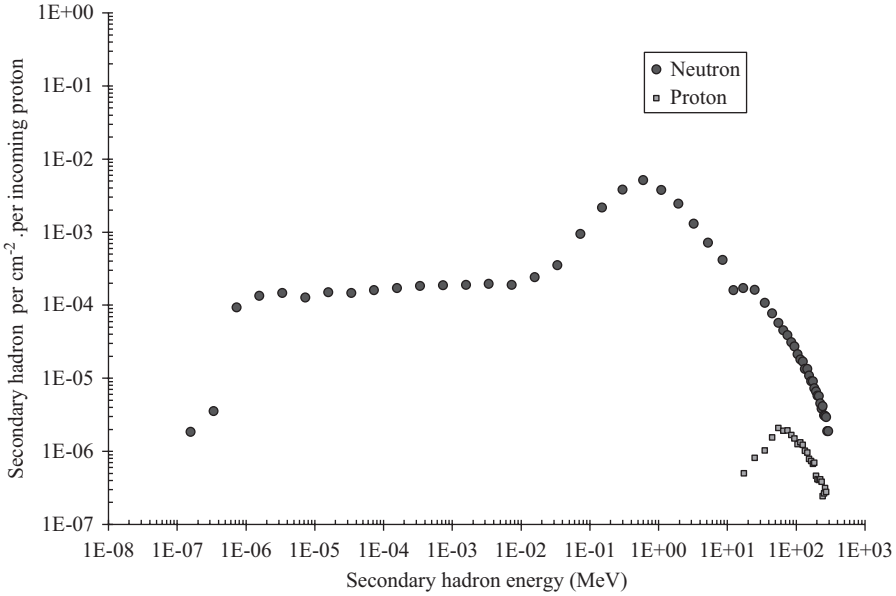


**Fig. 2.** Hadron fluence produced by Monte-Carlo simulations using the Dubna Cascade Model for the Pb (4-section U-blanket) target irradiated by relativistic proton beam.

**Table 1**
The effective cross section ($\sigma_{eff}$) as well as the fraction on the reaction rate of each applied radiators in specific energy ranges.

| Neutron | Slow neutron (up to 10 keV) | | Intermediate-fast neutron (0.3–3 MeV) | | Fast neutron (above 2 MeV) | |
|---|---|---|---|---|---|---|
| Reaction | $\sigma_{eff\ (b)}$ | Reaction rate (%) | $\sigma_{eff\ (b)}$ | Reaction rate (%) | $\sigma_{eff\ (b)}$ | Reaction rate (%) |
| Au(n,γ) | 194±29 | >99 | | | | |
| $^{238}$U(n,γ) | 29±4 | >95 | | | | |
| $^{114}$Cd(n,γ) | 1.5±0.2 | 50–60 | | | | |
| $^{10}$B(n,α) | 129±23 | >90 | | | | |
| H(n,n′) | | | 4.8±0.8 | 100 | | |
| $^{232}$Th(n,f) | | | | | 0.14±0.03 | 100 |

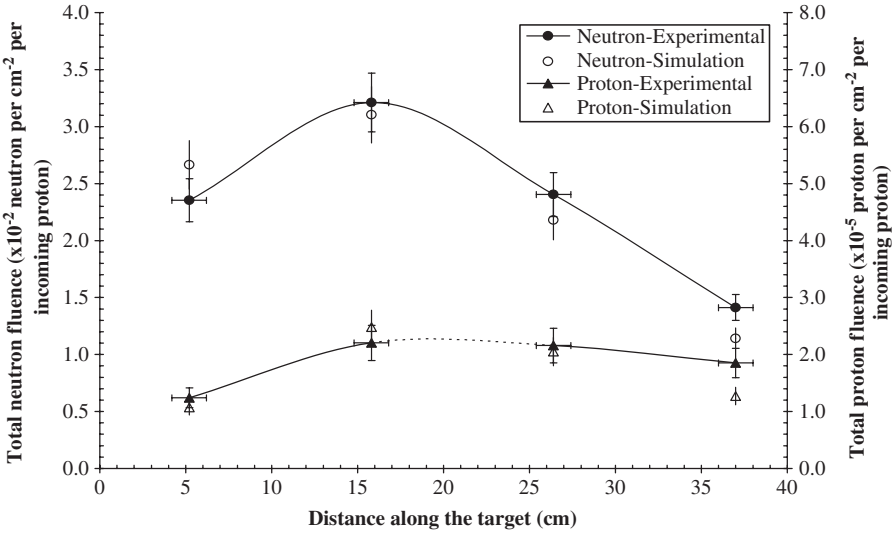


**Fig. 3.** Hadron spatial distribution measured over the Pb (U-blanket) target irradiated by a relativistic proton beam with energy 2 GeV (the lines are to guide the eye).

Similar conclusions were found concerning the MC simulation results. The total hadron spatial distribution experimentally determined over the U-blanket is presented in Fig. 3. Simulation results summarized for each isolethargic step up to neutron energy of 20 MeV are also shown in Fig. 3. Both neutron and proton production appeared to have an increasing behaviour with a maximum value over the second section of the U-blanket, followed by a decrease towards the target end. The decline of neutron production appeared to be more evident than proton production. Proton fluence remained quite constant from the second, up to the fourth section of U-blanket, within uncertainty of the experimentally obtained proton fluences. The simulated values were slightly lower than the experimental results but within $1\sigma$ for both sets of data. In the fourth section the difference between experimental and simulation data were $\leqslant 2\sigma$.

The experimentally determined and calculated total neutron fluence in the middle of each particular section was taken as representative of the entire section. The total neutron multiplicity was estimated by integration over the entire surface of each particular section of the U-blanket. The results are displayed as a function of the distance along the target in Fig. 4. The detailed analysis of the uncertainties contribution to the fluence measurements, for each detection technique, is presented on Table 2. The statistical error in the MC calculations was less than 4% for each isolethargic energy bin. Therefore, the overall uncertainty of the calculated neutron fluence varied from 9% up to 14% depending on the number of bins that are summarized for each neutron energy range.

The experimentally determined neutron multiplicities for every neutron energy range were compared to the simulation

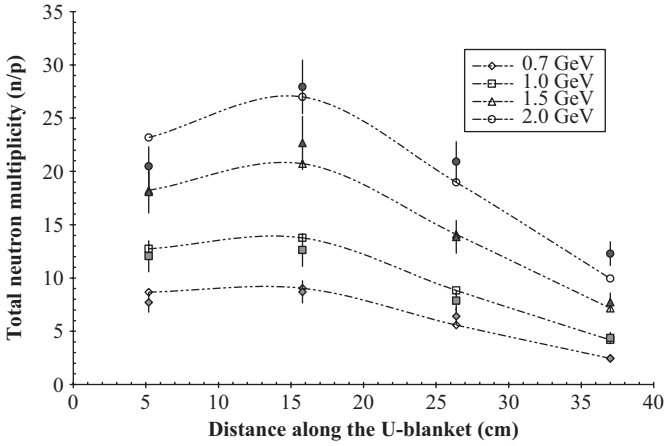


**Fig. 4.** Total neutron multiplicity determined using the complementary set of passive detectors (filled symbols) and calculated using the DCM–DEM simulation code (void symbols) over each section of the U-blanket (the lines are to guide the eye).

ones for each section of the U-blanket and for all studied proton beam energies (totally 48 pairs). The same comparison was made with the data over the second section of the U-blanket during the 1.5 GeV proton beam irradiation [33]. After four-year experience gained over the beam profile and fluence during short-term irradiations ($10^{11}$ protons) the experimental data as well as simulations were reprocessed. Detailed tables of neutron multiplicity are included in Appendix A. The mean value of the E/S ratio

**Table 2**
The uncertainties contribution (%) of the hadron fluence determination.

| Source of uncertainty | SSNTDetecors | Activation detectors |
|---|---|---|
| Radiator mass | ⩽4 | ⩽3 |
| Counting statistics | 8-17 | 1–8 |
| Radiator response and/or $\sigma_{eff}$ | 17–18 | 13–18 |
| Ge efficiency* $\gamma$-fraction | | ~3 |
| Beam intensity | 6–10 | 6–10 |
| Total | 20–27 | 15–22 |

was $1.15 \pm 0.22$ with 67% of the comparing pairs to be within $1\sigma$ of both uncertainties while between $2\sigma$ is the 90% of the comparisons. Simulation data using the MCNPX code over the second section of the U-blanket for an incoming proton beam 1.5 GeV [34,35] were also compared with the corresponding to DCM code and experimental results at the same position (Table A2). A fairly good agreement can be observed between both simulation codes and experimental results in the central target area.

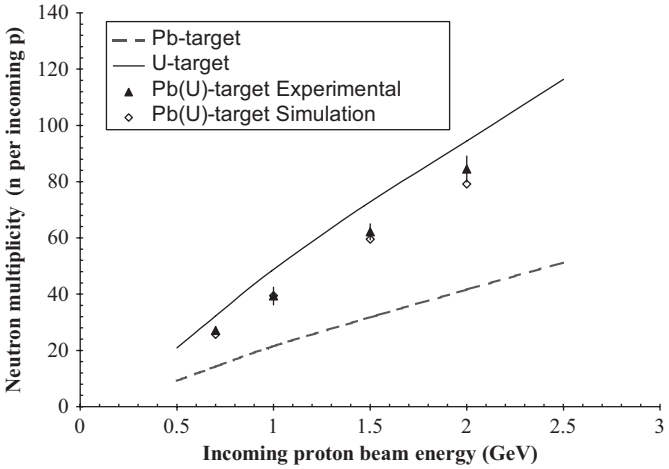


**Fig. 5.** Neutron multiplicity measured on the surface of the "Energy plus Transmutation" assembly in comparison with similar massive Pb and U targets.

### 3.2. Spallation source performance

The neutron multiplicities estimated using the experimental and the simulation results are presented in Fig. 5, as a function of proton beam energy. The same figure provides a comparison of the neutron multiplicity between current and previous studies on massive Pb or U spallation sources. The neutron multiplicity resulting from the specific set-up could be compared with the respective one from a massive Pb target with 20 cm in diameter and 60 cm in length [36,37]. Unfortunately, there are no available data on neutron multiplicity from a massive U target with the same dimensions as those of the current study. However, a number of comparative studies on U and Pb targets with different dimensions than the "E+T" [12,13,38], provide evidence that uranium produces about the double neutron yield than lead after been irradiated with relativistic proton beams [16]. That rule has been applied to the data obtained from a massive Pb target with 20 cm in diameter and 60 cm in length, in order to estimate the neutron multiplicity of a similar massive U target, Fig. 5.

The neutron multiplicity of the combined Pb/U-blanket spallation source appeared to approach the respective one of a massive U target, following similar energy increment with previous studies [1,2,13,37]. The energy required for the extraction of one neutron from the U-blanket surface ($\varepsilon$, MeV/n) decreased with proton beam energy increment. In the studied proton beam energies (0.7–2 GeV) the determined values follows a logarithmic function: $\varepsilon = 25.2(\pm 0.1) - 2.3(\pm 0.3) * \mathrm{Ln}(E_{p,GeV})$ within a 97% confidence level. Similar values were reported for an ADSystem whereat the spallation source was a U target inside a sub-critical reactor assembly (natural U robs and water moderator) [2]. The proton multiplicity was found to spread from $0.04 \pm 0.01$ up to $0.06 \pm 0.01$ per incoming proton, for proton beam energy ranging from 0.7 up to 2.0 GeV, respectively.

For all studied proton beam energies, the neutron multiplicity was $1.7 \pm 0.2$ times higher than the respective one measured on a Pb target using similar detection (threshold) technique [37]. According to the experimental results, the neutron excess per incoming proton produced by the uranium follows a linear energy increasing function: $n_{excess}/p_{incoming} = 21.1(\pm 0.5) * E_{p(GeV)} - 4.4$ $(\pm 0.7)$ within a 99% confidence level. This neutron excess was induced primarily by U($n_{sp}$, f) reaction in the fuel-blanket releasing 2.5 neutrons per fission. Therefore, in proton beam energy range from 0.7 up to 2.0 GeV, the fissions per incoming proton produced in the U-blanket spread between $4.4 \pm 0.6$ and $15 \pm 1$, respectively. These fission production amounts to energy amplification from 1.1 up to 1.4 ($\pm 0.2$) considering the energy released (180 MeV) per fission. In the studied proton beam energy range, the system sub-criticality, $k_{eff}$, had a mean value of $0.18 \pm 0.04$, taken into account the total neutron fluence measured on the surface of the U-blanket and the one after the shielding.

After 1 mm of Cd and 26 cm in thickness polyethylene shielding, the measured intermediate-fast neutron fluence (0.3–3 MeV) was about one order of magnitude less than the fluence produced from the source. According to the experimental data the slow neutron (<10 keV) fluence after the shielding was found to be similar to the intermediate-fast neutron fluence i.e. 1.1 $(\pm 0.2) \times 10^{-3}\,\mathrm{cm}^{-2}$ per incoming proton. The slow neutron fluence, measured on the surface of the U-blanket, was due to the backscattered neutrons from the shielding via (n,n′) reactions of the intermediate-fast neutrons coming from the source.

At the boundary layer between the U-blanket and the shielding the neutron spectrum via U(n,$\gamma$) reactions produced from 0.9 $(\pm 0.1)$ up to 2.8 $(\pm 0.3) \times 10^{-4}$ nuclei of $^{239}$Np per g of uranium and per incoming proton, for beam energy ranged from 0.7 up to 2 GeV, respectively. Using the specific spallation source in a hypothetical ADSystem with 10 mA proton beam, at the surface layer of U-blanket a $^{239}$Pu amount of $0.21 \pm 0.3\%$ per weight and per GeV of proton beam will be accumulated after one month of the ADS operation. The Pu production could be avoided by applying a variety of actinides, such as $^{232}$Th instead of uranium, around the Pb core [3]. A rather lower neutron multiplicity for a Th-blanket compared to U-blanket, is expected, since fission reactions dominate on neutron multiplication in the fuel while fast neutron fission cross-section of thorium is about the half compared to uranium.

Amounts of He and H are deposited in the system due to fast neutrons induced (n,$\alpha$) reactions and protons. According to the experimental results $10^{18}$ atoms of hydrogen per $\mathrm{cm}^3$ will be deposited at the near surface volume of the source after one month of the hypothetical ADS operation. At the same volume an amount of $10^{17}$ atoms of helium per $\mathrm{cm}^3$ and per month will be accumulated in a Fe-based structural material, considering the cross-section of Fe(n,$\alpha$) reaction 0.15 b [10]. The Pb core affected by more than one orders of magnitude more hydrogen due to the evaporated secondary protons that are trapped in the target. Possible adverse effects in the solid matter due gases [16] could be avoided by using a liquid target such as Hg.

## 4. Conclusion and perspectives

In the present study, relativistic proton beams were used to irradiate a sub-critical Pb/U-blanket electronuclear set-up surrounded by a polyethylene shielding. The neutron spectrum emitted by the Pb core effectively incinerated the U-blanket producing a neutron excess due to $6.1 \pm 0.8$ up to $7.5 \pm 0.9$ fissions per incoming proton and per GeV of beam energy ranged from 0.7 up to 2.0 GeV, respectively. The hard neutron fluence produced by the source reduced though the shielding by one order of magnitude. A slow neutron component was provided at the U-blanket surface due to backscattered neutrons by the shielding. In a hypothetical ADSystem operating with a relativistic proton beam at 10 mA, the slow neutrons production rate, $10^{17}\,s^{-1}$, would results to a substantial transmutation rate through $(n,\gamma)$ reactions. An amount of $2.1 \pm 0.3$ mg of $^{239}Pu$ per g of uranium and GeV of proton beam is expected to be accumulated at the surface of the U-blanket after one month of ADS operation. Except transmutation, the slow neutron rate could also be used for incineration of $^{239}Pu$ via fission reactions. The intermediate-fast neutron rate, $10^{18}\,s^{-1}$, could also be effectively used to incinerate minor actinides. The sub-criticality of the system could be increased by increasing the neutron excess, due to the U-blanket, while decreasing the neutron loss. Amounts of Np, Pu, Am and Cm isotopes could also be used to enrich the blanket especially at the surface layer in order to achieve their higher burn-up process compared to uranium, through fission reactions induced by intermediate and slow neutrons. In real operation conditions, the spallation source should be encased in a more sophisticated shielding, like a reactor-type moderator/"reflector", in which an efficient transmutation rate of long-lived fission products could be achieved as well.

## Acknowledgements

The authors are grateful to Professor A.I. Malakhov and the staff of the Laboratory of High Energies, JINR Dubna, for their continuous support to our work. Special gratitude is due to Professor A.D. Kovalenko and the operation crew of the Nuclotron accelerator for providing high-intensity beams during irradiations.

## Appendix A

The neutron fluences at different energy ranges determined over each section of the U-blanket using passive methods (total uncertainty 15–27%) and calculated values using Monte Carlo simulation codes (overall uncertainty 9–14%) for all studied proton beam energies (see Tables A1–A4).

**Table A1**
Neutron multiplicity (n/p) over first section U-blanket.

| Neutron energy range | 0.7 GeV protons | | 1.0 GeV protons | | 1.5 GeV protons | | 2.0 GeV protons | |
|---|---|---|---|---|---|---|---|---|
| | DCM code | Measured | DCM code | Measured | DCM code | Measured | DCM code | Measured |
| Up to 10 keV | 0.8 | 0.8 | 1.2 | 1.1 | 1.7 | 1.9 | 2.2 | 2.2 |
| 0.3–3 MeV | 4.8 | 4.9 | 7.0 | 8.0 | 9.9 | 12.0 | 12.5 | 13.1 |
| Above 2 MeV | 2.1 | 2.0 | 3.1 | 3.0 | 4.5 | 4.2 | 5.7 | 5.3 |

**Table A2**
Neutron multiplicity (n/p) over second section U-blanket.

| Neutron energy range | 0.7 GeV protons | | 1.0 GeV protons | | 1.5 GeV protons | | | 2.0 GeV protons | |
|---|---|---|---|---|---|---|---|---|---|
| | DCM code | Measured | DCM code | Measured | MCNPX code | DCM code | Measured | DCM code | Measured |
| Up to 10 keV | 0.9 | 1.0 | 1.3 | 1.5 | 2.1 | 2.0 | 1.9 | 2.6 | 2.5 |
| 0.3–3 MeV | 4.8 | 5.0 | 7.4 | 7.5 | 11.7 | 11.0 | 16.6 | 14.3 | 19.7 |
| Above 2 MeV | 2.0 | 2.8 | 3.1 | 3.6 | 4.3 | 4.7 | 4.1 | 6.1 | 5.7 |

**Table A3**
Neutron multiplicity (n/p) over third section U-blanket.

| Neutron energy range | 0.7 GeV protons | | 1.0 GeV protons | | 1.5 GeV protons | | 2.0 GeV protons | |
|---|---|---|---|---|---|---|---|---|
| | DCM code | Measured | DCM code | Measured | DCM code | Measured | DCM code | Measured |
| Up to 10 keV | 0.7 | 0.7 | 1.1 | 1.0 | 1.7 | 1.8 | 2.3 | 2.3 |
| 0.3–3 MeV | 2.8 | 3.6 | 4.5 | 4.7 | 7.1 | 8.9 | 9.7 | 14.1 |
| above 2 MeV | 1.1 | 2.1 | 1.8 | 2.2 | 2.9 | 3.1 | 4.0 | 4.4 |

**Table A4**
Neutron multiplicity (n/p) over fourth section U-blanket.

| Neutron energy range | 0.7 GeV protons | | 1.0 GeV protons | | 1.5 GeV protons | | 2.0 GeV protons | |
|---|---|---|---|---|---|---|---|---|
| | DCM code | Measured | DCM code | Measured | DCM code | Measured | DCM code | Measured |
| Up to 10 keV | 0.5 | 0.5 | 0.7 | 0.8 | 1.1 | 1.4 | 1.5 | 1.7 |
| 0.3–3 MeV | 1.1 | 1.5 | 2.0 | 2.9 | 3.5 | 4.6 | 4.8 | 8.0 |
| Above 2 MeV | 0.4 | 0.5 | 0.8 | 0.7 | 1.5 | 1.7 | 2.1 | 2.5 |

## References


[1] C.D. Bowman, et al., Nucl. Instr. and Meth. Phys. Res. A 320 (1992) 336.
[2] F. Carminati, et al., Report CERN/AT/93-47 (ET), 1993.
[3] S. Andriamonje, et al., Phys. Lett. B 348 (1995) 697.
[4] M.I. Krivopustov, et al., J. Radioanal. Nucl. Chem. 222 (1997) 267.
[5] J.S. Wan, et al., Kerntechnik 63 (1998) 167.
[6] R. Brandt, et al., Radiat. Meas. 31 (1999) 497.
[7] M.I. Krivopustov, et al., Kerntechnik 68 (2003) 48.
[8] A. Sinha, Nucl. Instr. and Meth. Phys. Res. A 274 (1989) 563.
[9] D. Hilscher, et al., J. Nucl. Mater. 296 (2001) 83.
[10] P. Jung, J. Nucl. Mater. 301 (2001) 15.
[11] B.M. Oliver, et al., J. Nucl. Mater. 307–311 (2001) 1471.
[12] L. Pienkowski, et al., Phys. Rev. C 56 (1997) 1909.
[13] D. Hilscher, et al., Nucl. Instr. and Meth. Phys. Res. A 414 (1998) 100.
[14] J.M. Carpenter, et al., Physica B 270 (1999) 272.
[15] A. Letourneau, et al., Nucl. Instr. and Meth. Phys. Res. B 170 (2000) 299.
[16] G.S. Bauer, Nucl. Instr. and Meth. Phys. Res. A 463 (2001) 505.
[17] S. Leray, et al., Phys. Rev. C 65 (2002) 044621(1–17).
[18] K. van der Meer, et al., Nucl. Instr. and Meth. Phys. Res. B 217 (2004) 202.
[19] J. Adam, et al., Am. Inst. Phys. Conf. Proc. 769 (2004) 1560.
[20] M. Krivopustov, et al., JINR Preprint E1-2004-79, 2004.
[21] A. Krása, et al., JINR Preprint E1-2005-46, 2005.
[22] M. Zamani, et al., Radiat. Meas. 26 (1996) 87.
[23] J.R. Harvey, et al., Radiat. Prot. Dosim. 77 (1998) 267.
[24] G. Remy, et al., J. Phys. 31 (1970) 27.
[25] S. Stoulos, et al., Appl. Radiat. Isot. 58 (2003) 169.
[26] M. Manolopoulou, et al., Nucl. Instr. and Meth. Phys. Res. A 586 (2008) 239.
[27] A.D. Kovalenko, et al., JINR Rapid Communications No 1[64], 1994.
[28] A.N. Sosnin, et al., Izv. RAS, Phys. Ser. 66 (2002) 1494.
[29] ENDF/B-*x* and the references within, 〈http://www.nndc.bnl.gov〉.
[30] F.M. Nortier, et al., Appl. Radiat. Isot. 41 (1990) 1201.
[31] F. Tárkányi, et al., Nucl. Instr. and Meth. Phys. Res. B 245 (2006) 379.
[32] W.J. Nieckarz, A.A. Caretto Jr., Phys. Rev. 178 (1969) 1887.
[33] S. Stoulos, et al., Nucl. Instr. and Meth. Phys. Res. A 519 (2004) 651.
[34] S.R. Hashemi-Nezhad, et al., Nucl. Instr. and Meth. Phys. Res. A 591 (2008) 517.
[35] M. Majerle, et al., JINR Preprint E15-2007-82, 2007.
[36] R.G. Vasil'kov, et al., At. Energ. 25 (1968) 479.
[37] R.G. Valsil'kov, V.I. Yurevich, ICANS-XI, KEK (1990) 340.
[38] J.S. Fraser, et al., Phys. Can. 21 (1965) 17.